Molecule-Scale Diffusion in Polyether Hybrid Cobalt Bipyridine Molten Salts

Joseph C. Crooker and Royce W. Murray*

Kenan Laboratories of Chemistry, University of North Carolina, Chapel Hill, North Carolina 27599-3290

Received: February 16, 2001; In Final Form: May 31, 2001

Microband voltammetry is described in undiluted molten salts of Co(II) bipyridine complexes to which short ($n = 1$, 2, or 3 units) polypropylene oxide oligomers have been appended. It has been possible to measure cyclic voltammetric and potential step responses under conditions where the diffusion layer thickness formed in the electrolysis is demonstrably less than the diameter of the Co complex. Apparent diffusion coefficients recorded in the molecule-scale diffusion regime as a function of n and temperature range from 1×10^{-14} to 1×10^{-18} cm^2/s. The corresponding bulk diffusion coefficients are ca. 7-fold smaller. The peculiar shape of the current−time response is rationalized as a "finite-diffusion" effect. Analysis of potential-step current−time results as the kinetics of a first-order electron transfer oxidation (of complexes adjacent to the electrode) gives rate constants quantitatively equal to the diffusion rate results, provided the latter are divided by the (Co complex diameter)^2 as the characteristic hopping distance of the interfacial electrochemistry. The kinetic data also agree with cyclic voltammetry rate constants if the difference in over-potential is taken into account.

This laboratory has for several years used[1] electrochemical voltammetry to investigate semisolid materials that are basically undiluted redox species in an amorphous state. Other groups have also contributed to this area.[2] We have sought to establish methodology that successfully copes with the extremely slow mass and charge transport phenomena characteristic of semisolids and to design chemical materials whose study will shed light on the transport dynamics of semisolid phases and which have "soft-material" properties conducive to making reproducible quantitative contact to a solid electrode. Our current design strategy—attaching oligomeric polyether chains to redox substances or to their counterions—has been effective and has led to room-temperature redox melts ranging from metal bipyridine complexes[1a,3] to ferrocene[1b] to perylene[1g] to metalloporphyrins[1c,d] to viologens[1h] to DNA.[1i]

This report presents measurements on a molten salt that probe the very limit of slow diffusive mass transport. The root mean-square diffusion length (L) of a species with diffusion coefficient D during a random walk[3] of duration t is $\approx [2Dt]^{1/2}$. Here, we describe experiments in which the average distances L over which an electrode reactant diffuses to an electrode demonstrably range from multiples to fractions of the physical dimension δ_D (diameter) of the diffusant itself (i.e., $\delta_D \leq L \leq \delta_D$). We call the latter situation "molecule-scale diffusion". Little is known about diffusion processes culminating in a chemical reaction in cases where the diffusion distance is extremely short, yet they have to be common, for example at reactive solid−solid interfaces.[4]

The molecule-scale diffusion measurements are based on perchlorate molten salts of Co(II) bipyridine complexes to which short (1, 2, or 3 units) polypropylene oxide oligomers have been appended.

These materials, although extremely viscous and with low polyether content, do not crystallize since the polyether chains are diasteromeric mixtures.[5] They are abbreviated as $Co(P_NM)_3$ where $n = 1$, 2, or 3; their perchlorate counterion is understood to be present throughout this paper. A fourth melt studied was

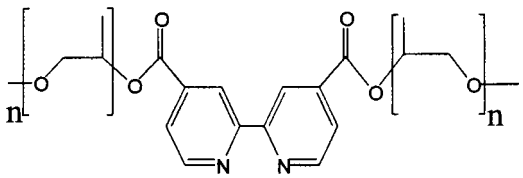

n	abbrev.
1	PM
2	P_2M
3	P_3M

an equimolar mixture of the $n = 1$ and $n = 2$ complexes, designated $Co(P_{1+2}M)_3$. In a preliminary report,[6] we were able to approach, but not fully achieve, the molecule-scale regime for $n = 3$; oxidation of the Co(II) complex was observed for diffusion pathlengths as short as $L \approx 2\ \delta_D$, where $\delta_D \approx 1.4$ nm. Our methodology in experiments on the $Co(P_NM)_3$ melts has since been refined and resistance effects subjugated, as recently described.[7]

Cyclic voltammetry and potential-step chronoamperometry are performed in the four *undiluted* $Co(P_NM)_3$ melts using lithographically defined microband electrodes[7] and at varied temperatures. Chronoamperometric currents measured at sufficiently long times such that $L > \delta_D$ (ordinary or "bulk" diffusion) follow Fick's laws and give diffusion coefficients (D_{bulk}) for the self-diffusion of the metal complex that range from 10^{-15} to 10^{-18} cm^2/s. Currents measured at shorter times are analyzed in three different ways. (*a*) When analyzed by Fickian relations, chronoamperometric current−time responses give apparent self-diffusion constants in the molecule-scale regime ($L \leq \delta_D$) that are slightly larger than D_{bulk}. (The molecule-scale diffusion regime is clearly an unusual one and we refer to it as "apparent" diffusion.) (*b*) The *same* chronoamperometric current−time responses are alternatively treated as reflecting the slow rate (s^{-1}) of a Co(II→III) heterogeneous electron-transfer reaction, being for electrolysis of metal com-

10.1021/jp010615y CCC: $20.00
Published on Web 07/13/2001

plexes that are already "at the electrode/melt interface" when the experiment is initiated. (*c*) Heterogeneous electron-transfer rate constants (cm/s) are obtained by analysis[3,8] of ΔE_{peak} values of cyclic voltammetry conducted in the molecule-scale regime. The results of these three data analyses, which have different dimensions but correspond to the *same* chemical event, can be related to one another using the metal complex dimension as the characteristic length scale of the interfacial dynamics, confirming a speculation of the previous report.[6]

Experimental Section

Synthesis of Co(P_3M), Co(P_2M), Co(PM). The published synthesis[7] of 2,2′-bipyridyl-4,4′-bis(tripropylene glycol monomethyl ether carboxylate), P_3M, was used for the ligands with $n = 1$ and 2 polypropylene oxide oligomers. Briefly, dimethyl bipyridine (Reilly) is oxidized to 4,4′-dicarboxy-2,2′-bipyridine with potassium permanganate under acidic reflux conditions, chlorinated with thionyl chloride (Fisher, used as received), and then ester-coupled to the tri- or di- or mono-propylene glycol monomethyl ether "tail" (Aldrich). Chromatographic procedures (silica gel with a 4:1 CH_2Cl_2:acetone solvent) remove mono-tailed products from the desired bitailed bipyridine ligand. NMR analysis[7] (acetone-d_6, Aldrich) confirms this via a 3:1 peak area ratio of the bipyridine ring protons to the proton alpha to the first ester group on the chain.

Four metal complexes Co(P_NM)$_3$ were prepared by mixing stoichiometric proportions of polyether-tailed ligand with Co$(ClO_4)_2 \cdot (H_2O)_6$ in anhydrous methanol. According to its NMR analysis,[7] the Co(P_3M)$_3$ melt contained a 5%(mol/mol) excess of cobalt perchlorate. The Co(P_2M)$_3$ melt contained a 1% excess of the P_2M ligand, and the Co(PM)$_3$ melt appeared to be stoichiometrically pure. The Co($P_{1+2}M$)$_3$ melt was a 50/50 mixture of the Co(PM)$_3$ and Co(P_2M)$_3$ melts. Since small amounts of excess ligand have a strong diffusion-plasticization effect on self-diffusion rates in Co(P_NM)$_3$ samples, the content of excess ligand was carefully measured by a proton NMR procedure.[7] An attempt was made to remove excess tailed ligand by repeated extraction of a CCl_4 solution with cyclohexane, but this procedure is only partly effective. Concentrations of the metal complex in the four melts were established[7] as 0.57, 0.71, 0.81, and 0.76 M, respectively, based on density measurements and assuming ideal stoichiometry.

Electrochemistry. Lithographically defined microband (LDM) electrodes[7] are placed into direct contact with the undiluted metal complex melts. The LDM electrodes consist of parallel, individually addressable 0.1 μm thick Pt films deposited atop an insulating Si/SiO_2 substrate and separated by 1.75 μm. The Pt films were either 2 mm long $\times$ 10 μm wide (LDM#1, $A = 2 \times 10^{-4}$ cm^2) or 0.5 mm long $\times$ 10 μm wide (LDM#2, $A = 5 \times 10^{-5}$ cm^2). One Pt film was used as the working electrode and the other as a pseudo-reference electrode. The reference electrode, although near the working electrode, remains outside[9] its (even smaller) diffusion field. A nearby 0.5 mm $\times$ 0.3 mm Pt pad on the Si/SiO_2 chip served as the counter electrode.[10] The LDM electrode design was crucial for these experiments; the microband working electrode with nearby reference is tolerant[9] of the extremely low ionic conductivities of the metal complex melts, and unlike microband electrodes fabricated in different ways, has a well-defined working area.

Films of the cobalt complex melts were cast onto the microelectrode assembly from a droplet of a solution in acetone. Polyether-tailed metal complexes tend to be hygroscopic (and imbibed moisture accelerates self-diffusion rates). The cast films were vacuum-dried at ca. 70 °C for at least 12 h, and vacuum was maintained throughout the experiments. The LDM electrodes were mounted on a locally built temperature-controlled (Lakeshore 330 autotuning temperature controller) vacuum stage and housed in a Faraday cage. Cyclic voltammetry and chronoamperometry were performed using a locally built, ultrasensitive potentiostat having current sensitivity down to a few tens of femtoamps. Experimental control was exercised with a PC interfaced with a Keithley DAS−HRES 16-bit A/D board, using locally written software.

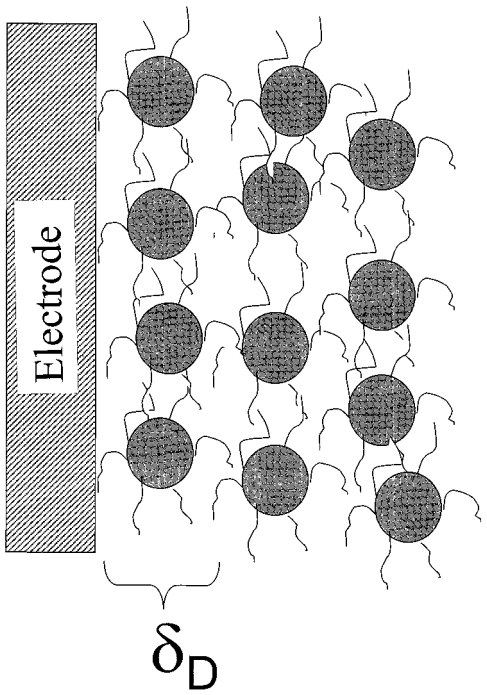

Figure 1. Cartoon of the first few monolayers of Co polyether-tailed complexes at the electrode surface. δ_D is molecular diameter.

Results and Discussion

We begin with a discussion of what is meant by molecule-scale diffusion. Figure 1 is a cartoon of an undiluted Co(II) redox phase next to the working electrode. The actual arrangement of Co(II) sites is not ordered as shown, but is disordered and dynamic. A continuing, slow, thermally activated, diffusive exchange of sites occurs laterally over the electrode surface and between adjacent monolayers of metal complexes. Despite this intrinsically random process, one can picture that, when an oxidizing potential is applied, a depletion layer of Co(II) sites forms as a quantity of sites equal to that *initially* in the first layer is oxidized, then a quantity equal to the second monolayer, and so on. Of course, the process does not actually occur in a perfectly stepwise layer-by-layer fashion, due to the concurrent diffusive exchanges.

The quantity of metal complex sites in the first monolayer (Γ_{mono}, mol/cm^2) is given by the product of site concentration and diameter (δ_D); the *charge* for a one-electron reaction of this quantity is denoted Q_{mono}. Values of experimental charge passed, relative to Q_{mono}, can thus be used as an experimental gauge to distinguish molecule-scale from more ordinary "bulk" diffusion. Molecule-scale diffusion of the Co(P_3M)$_3$ complex is discussed in terms of the *time* required to oxidize one equivalent monolayer ($\Gamma_{mono} = 8.2 \times 10^{-11}$ mol/cm^2) or less, i.e., the time required to pass a quantity of oxidative charge of amount less than or equal to the monolayer charge Q_{mono}. (In the context, for example, of using the microband working electrode LDM#2 ($A = 5 \times 10^{-5}$ cm^2), passing $\leq 4.0 \times 10^{-10}$

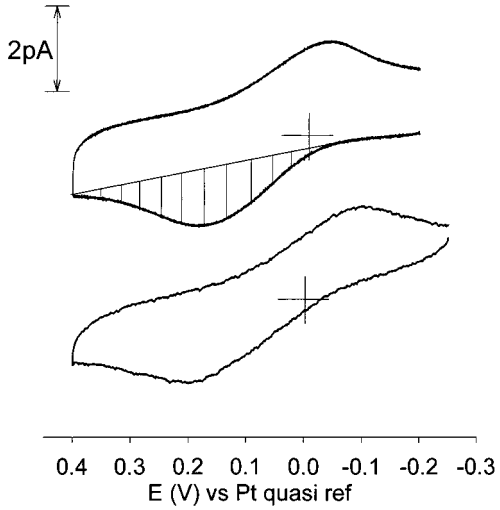

Figure 2. Cyclic voltammetry under molecule-scale diffusion conditions in $Co(P_NM)_3$ melts. Upper panel: $Co(P_3M)_3$ at 5 °C, LDM#2 microband electrode, $\upsilon = 1$ mV/s. Charge under hatched area is 2.9×10^{-10} C, which is 72% of the charge to oxidize one monolayer of this complex ($Q_{mono} = 4.0 \times 10^{-10}$C). (The baseline of the hatched area may underestimate the charge passed, but using a baseline extended from the current trace at −0.1V, which is probably an overestimate, still gives a charge (96%) less than that of a monolayer.) Lower panel: $Co(P_2M)_3$ at 25 °C, LDM#1 microband electrode, $\upsilon = 0.3$ mV/s.

C would correspond to the molecule-scale diffusion regime.) Molecule-scale diffusion is also discussed in terms of the diffusion *length* (i.e., depth of the diffusion layer) attained at times corresponding to having passed $\leq Q_{mono}$ of charge. In the context of Fickian diffusion, the depth L of the "diffusion layer" formed by the electrode reaction is $\approx[2Dt]^{1/2}$. Molecule-scale diffusion is the situation where $L \leq \delta_D$, where δ_D is the thickness of a monolayer of metal complex (its diameter). For the $Co(P_3M)_3$ complex ($\delta_D = 1.43$ nm), passing an oxidative charge equivalent to reaction of one-half of a monolayer of the $Co(P_3M)_3$ complex would correspond to a diffusion layer depth $L = 0.5\delta_D$.

It is worth mentioning three special attributes of the Co(II → III) bipyridine complex electron-transfer reaction that make it especially suitable for study of molecule-scale diffusion. First, the perchlorate counterion has been established,[1a] in analogous polyether-tailed Co(II) complex molten salts, as being much more diffusively mobile than the Co(II) complexes themselves; i.e., migration transport of the Co complex is unimportant. The rate of double-layer charging, by accumulation of perchlorate ions at the electrode/melt interface, is thus not a plausible rate-limiting step in the Co(II → III) reaction, at least under conditions where uncompensated resistance effects can be judged negligible.[11] Second, charge transport occurs solely by *physical* Co(II) site diffusion; the rates of Co(II → III) electron transfers are both slow and (third) are proportional[12] to the rate of physical diffusion (as expressed by D_{bulk}). The latter was described as a form of solvent dynamics control of the electron-transfer rate; we will find in the present work that the solvent dynamics control extends into the molecule-scale regime.

Molecule-Scale Diffusion in Cyclic Voltammetry. Figure 2 presents cyclic voltammetry in undiluted $Co(P_3M)_3$ (upper) and $Co(P_2M)_3$ (lower) metal complex melts. Even though the potential sweep rate is quite slow (the upper voltammogram was completed in ca. 20 min), the estimated charge under the voltammetric peaks is very small; that in the hatched area is 2.9×10^{-10} C. Given that $Q_{mono} = 4.0 \times 10^{-10}$ C, roughly 72% of a monolayer of $Co^{II}(P_3M)_3$ complex reacts during the

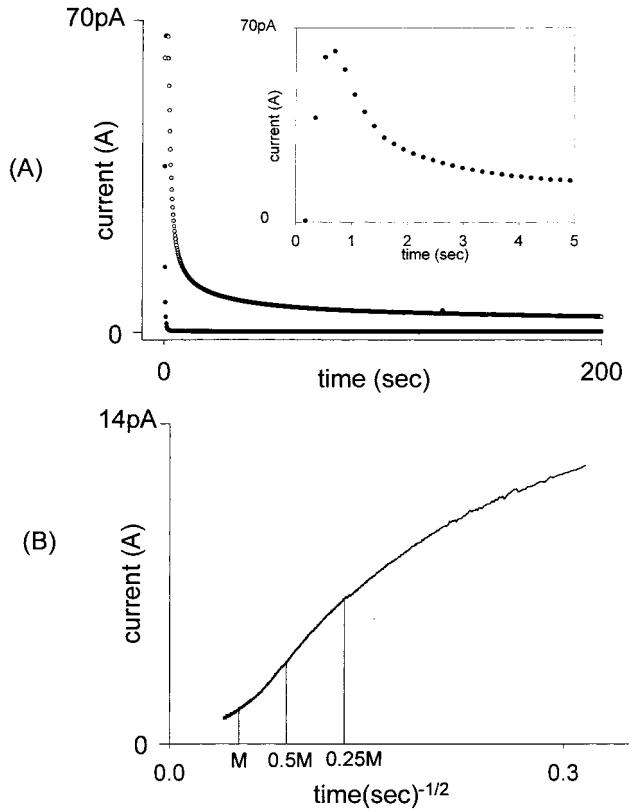

Figure 3. Panel A: (○) Chronoamperometric current−time response for a 500 mV potential step across the Co(II → III) wave for the $Co(P_2M)_3$ melt at 25 °C, LDM#1 microband electrode; (●) potential step in same melt but in double-layer background potential region where no faradaic reaction occurs. At 200 s in ○, the current is 6.7 pA; at the same time in ●, the current is 0.12 pA. Inset: short time currents in the $Co(P_2M)_3$ melt for the Co(II → III) reaction. Panel B: plot of eq 1 for the Co(II → III) current−time response in Figure 3A. The times marked are those at which the charge passed is equivalent to reaction of one-quarter (37 s, $0.25Q_{mono}$), one-half (112 s, $0.5Q_{mono}$), and one (590 s, Q_{mono}) monolayer of the metal complex. Slopes at these times give $D = 5.3 \times 10^{-17}$, 9.5×10^{-17}, and 2.5×10^{-17} cm²/s, respectively.

oxidative potential sweep. Analogous comparisons in the lower voltammogram show that roughly 54% of a monolayer of $Co^{II}(P_2M)_3$ complex reacted there.

As far as we are aware, Figure 2 presents the first examples of molecule-scale diffusion in cyclic voltammetry. The voltammograms have an otherwise qualitatively normal appearance. An analysis of the quasi-reversibility evident by their appreciable ΔE_{peak} values will be given below.

Molecule-Scale Diffusion in Chronoamperometry. *Diffusion Analysis.* Figure 3A shows an example current−time response (○) to a +500 mV chronoamperometric potential step across the Co(II→III) oxidation wave in the $Co(P_2M)_3$ melt, and a "background" potential step (●) taken in the double layer region (at more negative potentials) of the same melt. The diffusive process is analyzed with the current vs. $t^{-1/2}$ "Cottrell" plot shown in Figure 3B, according to the linear diffusion (chronoamperometry) relation[3]

$$i(t) = \frac{nFACD^{1/2}}{\pi^{1/2}t^{1/2}} \qquad (1)$$

where A is microband electrode area (2×10^{-4} cm² for the LDM#1 microband) and C is the concentration (mol/cm³) of Co(II) metal complexes in the melt. Currents are plotted only for times substantially exceeding the experimental cell time

TABLE 1: Comparison of Regression Analysis with Chronocoulometric Monolayer Analysis for $Co(P_NM)_3$ Melts at Various Temperatures

melt	temp (°C)	D_{bulk} (cm^2/s)[c]	$D_{0.5inflec}$ (cm^2/s)[c]	D_{inflec} (cm^2/s)[c]	$t_{0.5M}$ (sec)[d]	t_M (sec)[d]	t_{inflec} (sec)[d]	L_{inflec} (nm)[e]	L_M[i] (nm)[e]
$Co(P_3M)_3$[a]	25	2.3×10^{-15}	5.1×10^{-15}	9.6×10^{-15}	1.4	4.4	2.4	1.0	1.4
$C = 0.57$ M	20	6.7×10^{-16}	3.4×10^{-15}	5.2×10^{-15}	4.1	12	5.9	0.9	1.2
$\delta_D = 1.43$ nm[f]	15	4.1×10^{-16}	1.8×10^{-15}	3.2×10^{-15}	5.4	17	9.7	0.9	1.2
	10	1.8×10^{-16}	9.5×10^{-16}	1.6×10^{-15}	8.5	30	22	0.9	1.0
	5	1.6×10^{-16}	4.5×10^{-16}	8.6×10^{-16}	14	52	44	1.2	1.3
	0	1.2×10^{-16}	1.2×10^{-16}	3.5×10^{-16}	29	1.1×10^2	84	1.4	1.6
	−5	4.9×10^{-17}	6.3×10^{-17}	1.9×10^{-16}	62	2.1×10^2	2.0×10^2	1.4	1.4
	−18	9.0×10^{-19}	9.2×10^{-19}	4.6×10^{-18}	6.8×10^2	1.5×10^3	2.7×10^2	0.2	0.5
$Co(P_2M)_3$[b]	30	5.6×10^{-17}	1.2×10^{-16}	1.7×10^{-16}	55	2.9×10^2	51	0.8	1.8
$C = 0.71$ M	28	2.7×10^{-17}	8.2×10^{-17}	1.2×10^{-16}	80	4.6×10^2	86	0.7	1.6
$\delta_D = 1.33$ nm[f]	25	2.0×10^{-17}	5.3×10^{-17}	9.5×10^{-17}	1.1×10^2	5.9×10^2	1.2×10^2	0.7	1.1
	22	1.3×10^{-17}	3.2×10^{-17}	5.5×10^{-17}	2.0×10^2	$> 6 \times 10^2$[g]	2.2×10^2	0.8	[g]
$Co(P_{1+2}M)_3$[b]	55	2.2×10^{-16}	9.2×10^{-16}	1.0×10^{-15}	7.1	30	3.9	0.4	1.1
$C = 0.76$ M	50	6.6×10^{-17}	3.8×10^{-16}	4.7×10^{-16}	13	59	8.0	0.3	0.9
$\delta_D = 1.30$ nm[f]	45	7.9×10^{-17}	1.6×10^{-16}	1.6×10^{-16}	35	1.6×10^2	42	0.8	1.6
	40	2.2×10^{-17}	5.2×10^{-17}	5.9×10^{-17}	98	4.9×10^2	90	0.6	1.5
	35	2.8×10^{-17}	1.3×10^{-17}	2.8×10^{-17}	2.6×10^2	$> 6 \times 10^2$[g]	1.5×10^2	0.9	[g]
$Co(PM)_3$[a]	85	2.2×10^{-16}	1.7×10^{-15}	2.4×10^{-15}	8.5	24	7.0	0.6	1.0
$C = 0.81$ M	82	8.0×10^{-17}	1.0×10^{-15}	1.4×10^{-15}	6.5	34	5.3	0.3	0.7
$\delta_D = 1.27$ nm[f]	80	4.5×10^{-17}	8.7×10^{-16}	1.1×10^{-15}	5.3	43	7.0	0.2	0.6
	75	3.9×10^{-17}	5.3×10^{-16}	6.7×10^{-16}	4.3	69	14	0.3	0.7

[a] Analyzed with LDM#2 electrode ($A = 5 \times 10^{-5}$ cm^2). [b] Analyzed with LDM#1 electrode ($A = 2 \times 10^{-4}$ cm^2). [c] D_{bulk} calculated from Cottrell plot at times $\geq 2(t_{inflec})$. $D_{0.5inflec}$ and D_{inflec} taken from Cottrell plot slopes at $t_{0.5M}$ and t_M. [d] Time required for equivalent half-monolayer ($t_{0.5M}$) and monolayer (t_M) of charge (Q_{mono}) to pass; t_{inflec} is time of maximum slope of Cottrell plot. [e] $L_{inflec} = [2D_{bulk}\, t_{inflec}]^{1/2}$ and $L_M = [2D_{bulk}\, t_M]^{1/2}$. [f] Molecular diameter, as calculated from measured concentration assuming cubic packing. [g] The equivalent of a monolayer of charge (Q_{mono}) had not been electrolyzed by the end of the experiment (600 s).

constant, which is revealed as <1 s in the inset of Figure 3A. Note that all currents in the Figure 3A inset are at times shorter than the shortest time in the Cottrell plot in Figure 3B.

Figure 3B shows that, at the longest times (lower left), the Cottrell plot becomes linear and extrapolates to the origin, as required by eq 1 and as observed in previous experiments[1] under conditions producing "ordinary" diffusion layer thicknesses $L > \delta_D$. The slope of this segment of the Cottrell plot gives physical diffusion constants D_{bulk} that are given in Table 1 for measurements at different temperatures in the four Co complex melts. The D_{bulk} values, consistent with previous results,[1a,3,12] are quite small and decrease as the polyether chains are shortened because of the concurrent decrease of free volume.[1e] As a miscellaneous observation and to emphasize the slowness of the observed mass transport, the time required for a Co(II) complex with a D_{bulk} of 10^{-18} cm^2/s to diffuse a distance of 1 cm is ca. 6.3 billion years, a significant fraction of the age of the universe!

The chronoamperometric current−time curve in Figure 3A was integrated to give a charge−time response (Figure S-1) from which we could assess the times required for reaction of a monolayer (Q_{mono}), or a fraction thereof, of the Co(II) complex. The times 0.25 M, 0.5 M, and M marked on the Figure 3B Cottrell plot correspond to times at which $0.25Q_{mono}$, $0.5Q_{mono}$, and Q_{mono} charges had been passed. Clearly the major portion of the Figure 3B Cottrell plot lies in the molecule-scale regime and is the first result of this kind. Values of the times at which $0.5Q_{mono}$ and Q_{mono} charges had been passed ($t_{0.5M}$ and t_M, Table 1) vary by a factor of $>10^2$ for the different metal complex melts and temperatures.

The chronoamperometric current−time plot (Cottrell plot) in Figure 3B has an unusual shape that is typical of experiments under molecule-scale diffusion conditions (i.e., when $L \leq \delta_D$). At short times, the slope of the plot increases with increasing time, reaches a maximum (the inflection in the curve, at t_{inflec}), and then decreases until it becomes constant (the longest time, D_{bulk} segment). All of these changes in the Cottrell plot occur at times where less than Q_{mono} of charge has been passed. The time t_{inflec}, determined by differentiation (see Figure S-2), increases with decreasing melt temperature (Figure S-3), and with shorter polyether chains, just as do values of D_{bulk}. In fact, as seen in Table 1, the time t_{inflec}, throughout the melt experiments, is generally near that ($t_{0.5M}$) at which a charge of $0.5Q_{mono}$ has been passed.

The Cottrell plot inflection behavior in Figure 3B is clearly a molecule-scale diffusion transition region associated with passing roughly the first monolayer of charge. After passing roughly Q_{mono} of charge, Fickian properties are observed, as noted above. The apparent diffusion constants calculated from the Cottrell plot inflection times (and at one-half of that time, $0.5t_{inflec}$) are given in Table 1. The values of D_{inflec} are larger than the bulk diffusion constants D_{bulk}, but the ratio D_{inflec}/D_{bulk} is relatively constant 7(±4) over the nearly 10^4-fold range of diffusion rates. The larger value of D_{inflec} is examined later in this report.

The calculated diffusion length is another identifier of the molecule-scale diffusion regime. Table 1 shows values for the diffusional pathlength L_{inflec} calculated based on the time t_{inflec} and using D_{bulk} as the diffusion constant. We see that L_{inflec} is typically a fraction of the diameter of the Co complex. A similar result (L_M), again a fraction of the metal complex diameter δ_D, is obtained using the time t_M.

The apparent diffusion constants in the molecule-scale regime are thermally activated, as are those in the "bulk" regime (D_{bulk}). Activation plots in Figure 4 yield barrier energies of 126, 102, and 109 kJ/mol for diffusion constants evaluated at $t_{0.5mono}$, t_{inflec}, and in the bulk diffusion regime, respectively. The latter two values are indistinguishable from one another within the considerable scatter in the plots. The value for D_{bulk} is considerably larger than the ca. 80 kJ/mol previously observed

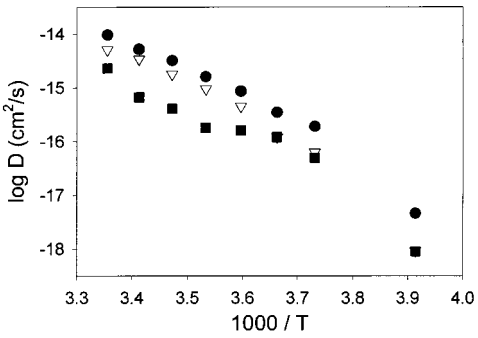

Figure 4. Activation plots of diffusion coefficients from Table 1 for $Co(P_3M)_3$ melt. Linear regression of $D_{0.5inflec}$ (▽), D_{inflec} (●), and D_{bulk} (■) plots gives activation barrier energies of 126, 109, and 102 kJ/mol, respectively.

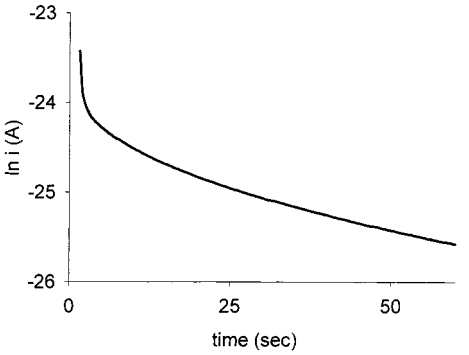

Figure 5. Plot of ln(current) versus time (1.5 s < time < 60 s) for the $Co(P_2M)_3$ melt at 30 °C, LDM#2 microband electrode. The slope at 51 s (ca. t_{inflec}) gives $k_{ET} = 0.016$ s^{-1}.

in our lab for a $Co(E_3M)_3$ (E = ethylene oxide) polyether-tailed cobalt bipyridine molten salt.[1a]

Electron-Transfer Rate Analysis, k^0. The first monolayer of Co complex does not react instantly in the potential step of Figure 3 because the Co(II → III) reaction rate is very slow. Current−time results such as those in Figure 3 can be analyzed for the kinetics of electron transfer between Co(II) complexes and the adjacent electrode; in the analysis we imagine that the reaction proceeds by all of the first monolayer reacting before any diffusive mixing steps occur with other Co complexes not initially in the first monolayer. The current−time data are plotted (Figure 5) as ln(current) vs. time, the slope of which is the electron-transfer rate constant (k_{ET}, s^{-1}) at the applied potential. This analysis is analogous to that of reactions of monolayers of redox sites *attached* to electrodes,[13] but is obviously an approximation; the Co(II) complexes are not actually attached to the electrode and can slowly diffuse. The curvature typical in these ln(current) vs. time plots (Figure 5, for the $Co(P_2M)_3$ complex) probably reflects the slow diffusional intermixing. Others[14] have discussed diffusion-controlled reactions with time-dependent rate constants following sudden perturbations (in this case the electrolysis step). The Figure 5 time-dependency may also be caused by the changing distribution of distances over time.

Electron-transfer rate constants k_{ET} were evaluated from the slopes at times t_{inflec} and $0.5t_{inflec}$; the results, given in Table 2, are the same within roughly 2-fold. These data are compared with the preceding diffusion analysis in a later section.

Analysis of Quasi-Reversible Cyclic Voltammetry. In the third data analysis, we return to cyclic voltammetry such as that portrayed in Figure 2. The results presented include some experiments in which the diffusion was not molecule-scale, but was close to it (several diameters of the Co(II) complex). In many cases, no reasonable cyclic voltammetry could be attained owing to the vanishingly small currents (<10 femtoamps) at the slow potential scan rates. The peak potential separation ΔE_{peak} was treated using the classical Nicholson−Shain method,[3,8] in which the measured value of ΔE_{peak} is equated to a theoretically computed kinetic parameter φ related to the electron transfer and diffusion rates by

$$\varphi = \frac{\left(\frac{D_0}{D_R}\right)^{\alpha/2} k^0_{cv}}{[D_0 \pi \nu (nF/RT)]^{1/2}} \qquad (2)$$

D_0 and D_R, the Co(III) and Co(II) diffusion coefficients, have been demonstrated[7] in D_{bulk} measurements to be equal in the Co complex melts. D_{bulk} values were employed in eq 2. We assume that the transfer coefficient $\alpha = 0.5$. ν is potential scan rate (V/s).

Results for the rate constant k^0_{cv} for the $Co(P_3M)_3$ and $Co(P_2M)_3$ complexes at different temperatures and potential scan rates are given in Table 3. There is no significant trend in the rate constant with potential scan rate (a typical test for the absence of iR_{unc} distortion of k^0_{cv}). The iR_{unc} effect in these melts has been discussed in detail[7] and shown, although not entirely negligible, to be minor.

The k^0_{cv} results in Table 3 correspond to the heterogeneous rate constant at the formal potential of the Co(II/III) couple. The rate constants determined using the first-order reaction plot in Figure 5, on the other hand, are at an applied over-potential of a few hundred mV and are larger.

Comparison of Molecule-Scale Diffusion Coefficients and Electron-Transfer Rates. That rates of electrochemical reactions are controlled by either the rate of reactants diffusing to the electrode or by their rates of electron transfer at the electrode is a fundamental concept[3] in the analysis of electrochemical experiments. If the time constant associated with reactant diffusion is slower than that associated with the electron-transfer reaction, then the current is controlled by reactant diffusion and is described by boundary value solutions to Fick's laws. If the

TABLE 2: Analysis of Molecule-Scale Diffusion as Electron Transfer Rate in $Co(P_NM)_3$ Melts at Various Temperatures

melt	temp (°C)	D_{inflec}/δ_D^2 (s^{-1})[a]	k_{ET} at t_{inflec} (s^{-1})[b]	$D_{0.5inflec}/\delta_D^2$ (s^{-1})[a]	k_{ET} at 0.5 t_{inflec} (s^{-1})[b]	$k^0_{cv}/\delta_D a$ (s^{-1})[a]
$Co(P_3M)_3$	25	0.49	0.28	0.26	0.48	0.047
	20	0.27	0.13	0.17	0.18	0.015
	15	0.16	0.08	0.092	0.11	0.0077
	10	0.082	0.039	0.048	0.054	0.0021
	5	0.044	0.019	0.023	0.024	0.0022
	0	0.018	0.0096	0.0061	0.011	0.00059
	−5	0.0097	0.0037	0.0032	0.0042	
	−18	0.00023	0.0012	0.00047	0.0013	
$Co(P_2M)_3$	30	0.0096	0.016	0.0067	0.023	0.00083
	28	0.0069	0.010	0.0046	0.014	0.00035
	25	0.0054	0.0077	0.0030	0.0099	0.00021
	22	0.0031	0.0044	0.0018	0.0056	
$Co(P_{1+2}M)_3$	55	0.059	0.15	0.054	0.31	
	50	0.028	0.077	0.022	0.13	
	45	0.0095	0.016	0.0095	0.028	
	40	0.0035	0.0074	0.0031	0.013	
	35	0.0017	0.0062	0.00077	0.0046	
$Co(PM)_3$	85	0.15	0.19	0.11	0.33	
	82	0.087	0.15	0.062	0.27	
	80	0.068	0.11	0.054	0.17	
	75	0.042	0.057	0.033	0.090	

[a] See Table 1 for t_{inflec} and δ_D for each melt. [b] k_{ET} represents slope of plot of ln(current) versus time at $t = t_{inflec}$ or $0.5t_{inflec}$.

TABLE 3: Cyclic Voltammetry Results for Heterogeneous Rate Constants for the Co(II → III) Reaction in $Co(P_3M)_3$ and $Co(P_2M)_3$ Melts

sample	temp (°C)	scan rate (mV/s)	ΔE_{peak} (mV)		$k^0_{cv} \times 10^{-10}$ cm/s
$Co(P_3M)_3$[a]	25	50	288	0.049	58
		20	195	0.13	94
		10	223	0.093	49
	20	10	239	0.072	21
	15	1	173	0.151	11
	10	1	247	0.063	3.0
	5	1	230	0.070	3.2
	0	1	339	0.021	0.85
$Co(P_2M)_3$[b]	30	1	331	0.037	0.85
		0.75	292	0.049	1.1
		0.5	272	0.059	1.1
		0.4	240	0.082	1.3
		0.3	239	0.084	1.2
	28	0.75	371	0.022	0.35
		0.5	327	0.035	0.44
		0.4	291	0.049	0.56
		0.3	286	0.051	0.50
	25	0.5	384	0.019	0.21
		0.4	364	0.023	0.23
		0.3	299	0.045	0.38

[a] Analyzed with the LDM#2 electrode ($A = 5 \times 10^{-5}$ cm^2). [b] Analyzed with the LDM#1 electrode ($A = 2 \times 10^{-4}$ cm^2).

reverse is true, then the current is controlled by an appropriate model of rate versus over-potential, such as the Butler−Volmer expression.[3]

In the context of molecule-scale diffusion, these two classical concepts are merged and *become equivalent descriptions of the reaction rate*. In classical diffusion theory, a diffusion coefficient is defined[15] as a product of a jump rate (s^{-1}) and a jump distance squared.[15] In molecule-scale diffusion, we hypothesize that the "diffusive" jump rate and the electron-transfer rate are equivalent, and further propose that the characteristic jump distance is the diameter of the reactant Co(II) complex (δ_D, listed in Table 1 for the various complexes). This proposal is evaluated in Table 2 by dividing the results for $D_{0.5inflec}$ and D_{inflec} (Table 1) by δ_D^2. Compared to the results for k_{ET} at $t_{0.5inflec}$ and t_{inflec}, D_{inflec}/δ_D^2 is, over a range of 10^3 in the actual values, in nearly all cases the same within a factor of 2-fold. (The comparison at 0.5 t_{inflec} is not as close.) The similarity of D_{inflec}/δ_D^2 and k_{ET} values emphasizes that the diffusion and electron-transfer kinetic concepts converge in the molecule-scale diffusion regime, and that the optimum time for the comparison in the context of the chronoamperometric experiment is t_{inflec}.

The k_{ET} values of Table 2 are obtained at potentials between 0.1 and 0.2 V more positive than the formal potential of the Co(III/II) couple. The k^0_{cv} results in Table 3 are taken at the Co(III/II) formal potential. The k^0_{cv} results are compared in Table 2 to the cyclic voltammetry rate constants, k^0_{cv} (cm/s), by dividing the latter by the characteristic dimension δ_D. Table 2 shows that the ratio k^0_{cv}/δ_D closely parallels the D_{inflec}/δ_D^2 and k_{ET} values, but is as expected from the difference in potential, uniformly smaller, by an average factor of 12 ± 6. This factor corresponds (assuming $\alpha = 0.5$) to an over-potential of about 0.13 V, which is consistent with the actual experimental step potential noted above. In addition, the activation barriers of these parameters are similar (Figure S-4): 111, 84, and 109 kJ/mol for k^0_{cv}/δ_D, k_{ET}, and D_{inflec}/δ_D^2, respectively.

Properties of Molecule-Scale Diffusion. One can pose a host of questions regarding the chemical nature of the electrode−melt interface. First, are there specific chemical interactions between the cobalt complexes and the electrode? Is the ion-pairing[16] of the Co complex cation with its perchlorate counterion in these highly concentrated melts stronger or weaker at the interface versus the bulk? If either of these is significant, the diffusive hopping rates between the first and second monolayers (versus second and third) of Co complexes might differ. The bulklike value of D_{phys} that is reached after only Q_{mono} of charge (Figure 3) would suggest that this is not the case, or at least that any difference is small. We would also point to the somewhat remarkable fact that the molecule-scale diffusion results of Figures 2, 3, and 6 follow Fickian mathematics. One would anticipate that a particle should be required to undergo a much larger number of diffusive "hops" than one, to reproduce the random walk properties intrinsic in the Fick's Laws[3] on which eqs 1−3 are based. Our qualitative, intuitive rationale for this is that while any given Co complex may undergo only one or two diffusive hops during the experiment, observing a huge ensemble of complexes simultaneously doing this produces the effect of a much longer random walk process.

Second, the perchlorate counterion is not only more mobile than the metal complex,[1a] but it is also smaller, so that its distance of closest approach to the electrode can be less, which may distort the interfacial potential gradient that the complex itself actually experiences. It is not clear how to assess this issue from the present results.

Third, the data allow a conclusion with respect to previous results[12] for heterogeneous rate constants k^0_{cv} obtained for the Co(III/II) electron transfer under "normal" diffusion conditions (i.e., $L \gg \delta_D$). We observed[12] that in melt combinations of $[Co(bpy)_3]^{2+}$ complexes and polyethers, the self-diffusion coefficients of the Co complexes are *proportional* to k^0_{cv} and inversely proportional to viscosity over a remarkably wide, 10^{11}-fold range. This proportionality was interpreted to reflect "solvent dynamics" control of the rate of the Co(III/II) reaction. That the Co(III/II) reaction of the $Co(bpy)_3]^{2+}$ complex can be solvent-dynamics controlled in an organic matrix was recently[17] verified by high pressure measurements. The results for heterogeneous rate constants in Table 3 are entirely consistent with these earlier results, in that they fall (at the slowest end) onto the reported D_{phys} vs. k^0_{cv} plot,[12] within uncertainties no greater than any other segment of that plot. This correspondence strongly infers that electron transfer solvent dynamics control extends into the molecule-scale diffusion regime. Thus, slow nuclear motions of the same variety as those that control physical self-diffusion hops of the Co complex in the bulk melt also control the solvent-environment relaxation time constant of electrode-adjacent Co complexes, and in turn control the electron-transfer rate constant of those complexes.

Fourth, what is the origin of the peculiar inflection that appears in Cottrell plots such as that in Figure 3B? For potential step results, the inflection is characteristic of the molecule-scale diffusion regime. This unusual behavior can be rationalized by a diffusion concept known as "finite diffusion". Finite diffusion effects have been explored in electrochemistry in the contexts of thin layer electrochemical cells[18] and of electrolysis of thin films of redox polymers[19] and nanoparticles[20] on electrodes. In these earlier experiments, at early times in a potential step electrolysis, the diffusion layer (the reactant's depletion layer) is thin enough to lie entirely within the thin reactant film, so that the diffusion is so-called "semi-infinite". The Cottrell relation (eq 1) is derived under the assumption of semi-infinite diffusion. At longer electrolysis times, however, the thickening diffusion layer encounters the boundary at which the population of reactant disappears. Then the reactant flux to the electrode (i.e., the current) becomes depressed and eventually falls to zero as all of the reactant is consumed.

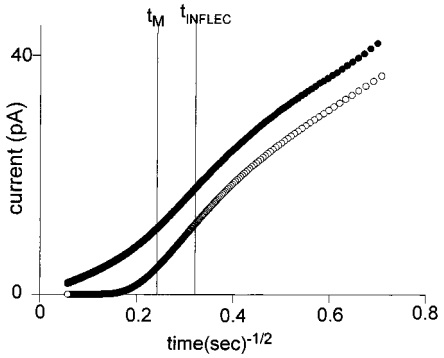

Figure 6. Experimental (●, offset upward by 5.3 pA, for clarity) and simulated (○) Cottrell plots (2s < time < 600 s) for the $Co(P_3M)_3$ melt at 15 °C (see Table 1). Simulated plot is from eq 3 based on (experimental values) $C = 5.7 \times 10^{-3}$ mol/cm^3, $A = 5 \times 10^{-5}$ cm^2, and d (δ_D) = 1.43 nm. Diffusion coefficient used for fit was 1.1×10^{-15} cm^2/s; this value is intermediate between the measured $D_{bulk} = 4.1 \times 10^{-16}$ cm^2/s and $D_{inflec} = 3.2 \times 10^{-15}$ cm^2/s in this melt.

In the context of "finite diffusion" in molecule-scale diffusion, the "thin reactant layer" would be the monomolecular layer of Co(II) complex initially next to the electrode. Figure 6 compares Cottrell plots for an experimental current−time response and for a calculated current−time response under finite diffusion conditions, according to the equation

$$i = \frac{nFAD^{1/2}C}{\pi^{1/2}t^{1/2}}\left[\sum_{k=0}^{\infty}(-1)^k\left\{\exp\left(\frac{-k^2d^2}{Dt}\right)-\exp\left(\frac{-(k+1^2)d^2}{Dt}\right)\right\}\right] \quad (3)$$

The curve is calculated using parameters (figure legend) corresponding to molecule-scale "diffusion" within a thin layer cell of thickness $d = \delta_D$ (the Co complex diameter). The calculated curve displays an inflection in slope and is strikingly similar in shape and scale to the experimental one. The main difference is an expected one; in the real melt, at longer times, rather than falling to zero, current continues to flow because electroactive species slowly diffuse into the fictitious "monolayer" thin layer cell, δ_D. We believe the finite-diffusion effect is a plausible general explanation for the behavior of the currents as the reaction passes through the molecule-scale diffusion regime.

Fifth, another factor to be considered in monolayer-scale diffusion is whether, owing to the longtime scale of the first monolayer's electrolysis, some electron transfers might occur over a longer distance. Electron tunneling rates vary exponentially with reactant separation times an electronic coupling term (β, ca. 1 Å^{-1}).[21] When concentrations are large, and diffusion to the electrode surface is very slow, Feldberg[22] has pointed out that electron transfer between electrode and reactant might occur at noncontact distances. A dimensionless parameter used to predict the likelihood of such reactions is

$$k^* = \frac{k_{S,0,E}\delta^2}{D} \quad (4)$$

where $k_{S,0,E}$ is the electron-transfer rate constant (s^{-1}) for reactions that occur in contact with the electrode surface. To observe a significant rate of extended electron transfer (which gives enhanced currents because a wider zone of material reacts), the simulations[22] show that k^* must be >1. In the present case, we calculate for example, for the $Co(P_3M)_3$ melt at 25 °C ($D_{bulk} = 2.3 \times 10^{-15}$ cm^2/s, $k^0 = 6.7 \times 10^{-9}$ cm/s), that $k^* = 0.029$. Similarly, for the $Co(P_2M)_3$ melt at 25 °C ($D_{bulk} = 2.0 \times 10^{-17}$ cm^2/s, $k^0_{cv} = 2.0 \times 10^{-11}$ cm/s), $k^* = 0.010$. Both values are substantially <1, an answer not supporting any contribution of extended electron transfer in the current molecule-scale diffusion system. The primary reason is that although D is very small, so is k^0_{cv}. One can infer, additionally, that extended electron transfer will in general, not occur for a reaction with solvent dynamics-controlled rates.

Finally, whether "molecule-scale diffusion" might be accessed using molecular systems that are not semisolids (with their extremely small D values) depends on a number of factors. In dilute solutions of small molecules in fluid solvents, for example, ferrocene in acetonitrile ($D = 2.3 \times 10^{-5}$ cm^2/s and $\delta_D \approx 0.5$ nm), the required molecule-scale diffusion electrolysis measurement time would be $t_{msd} \approx 50$ ps. Although (through microelectrodes) great strides have been made in the timescale of electrochemical experiments, this time seems beyond the current reach. On the other hand, the value of t_{msd} is rather sensitive to the reactant size; an increase in δ_D to 4 nm (in the same solvent so that D decreases by 8-fold) would amount to an 8^3 change in t_{msd} to ≈ 28 ns, which seems more achievable. Searching for molecule-scale diffusion with bulky reactants might thus be productive.

Acknowledgment. This research was supported in part by grants from the Department of Energy and the Office of Naval Research.

Supporting Information Available: Figures showing illustrative integration of chronoamperometric current−time responses to determine t_M, differentiation of Cottrell plots to determine t_{inflec}, Cottrell plots showing how t_{inflec} changes with temperature, and activation plots for electron-transfer kinetic data. This material is available free of charge via the Internet at http://pubs.acs.org.

List of Symbols

L	root mean-square diffusion distance
δ_D	molecular diameter
D_{bulk}	diffusion coefficient characteristic of bulk properties
Q_{mono}	charge (C) associated with reaction of a monolayer of the metal complex
t_M	time required to pass Q_{mono} charge
t_{inflec}	time of maximum inflection observed in Cottrell plots
L_{inflec}	root mean-square diffusion distance at time = t_{inflec}
L_M	root mean-square diffusion distance at time = t_M
k_{ET}	first-order electron-transfer rate constant (s^{-1})
k^0_{cv}	heterogeneous electron-transfer rate constant calculated via cyclic voltammetry (cm/s)

References and Notes

(1) (a) Williams, M. E.; Masui, H.; Long, J.; Malik, J.; Murray, R. W. *J. Am. Chem. Soc.* **1997**, *119*, 1997. (b) Pinkerton, M.; Le Mest, L.; Zhang, H.; Watanabe, M.; Murray, R. W. *J. Am. Chem. Soc.* **1990**, *112*, *3730*. (c) Velázquez, C. S.; Hutchison, J. E.; Murray, R. W. *J. Am. Chem. Soc.* **1993**, *115*, 7896. (d) Dickinson V, E.; Williams, M. E.; Hendrickson, S. M.; Masui, H.; Murray, R. W. *J. Am. Chem. Soc.* **1999**, *121*, 613. (e) Dickinson V, E.; Masui, H.; Williams, M. E.; Murray, R. W. *J. Phys. Chem.* **1999**, *103*, 11028. (f) Kulesza, P. J.; Dickinson V, E.; Williams, M. E.; Hendrickson, S.; Murray, R. W. *J. Phys. Chem. B* **2001**. *105*, 5833. (g) Williams M. E.; Murray, R. W. *Chem. Mater.* **1998**, *11*, 3603. (h) Hatazawa, T.; Terrill, R. H.; Murray, R. W. *Anal. Chem.* **1996**, *68*, 597. (i) Leone, A. M.; Weatherly, S. J.; Williams, M. E.; Thorp, H. H.; Murray, R. W. *J. Am. Chem. Soc.* **123**, *218*.

(2) Kulesza, P. J.; Malik, M. A. Solid State Voltammetry, in *Interfacial Electrochemistry Theory, Experiment, and Applications*; Wieckowski, A., Ed.; Marcel Dekker: New York, 1999; Chapter 37.

(3) Bard, A. J.; Faulkner, L. R. *Electrochemical Methods Fundamentals and Applications*; John Wiley & Sons: New York, 2001.

(4) *Solid State Electrochemistry*; Gellings, P. J., Bouwmeester, H. J. M., Eds.; CRC Press: Boca Raton, 1997.

(5) Analogous complexes based on polyethylene oxide chains of these very short lengths tend to crystallize after some time.

(6) Poupart, M. W.; Velazquez, C. S.; Hassett, K.; Porat, Z.; Haas, O.; Terrill, R. H.; Murray, R. W. *J. Am. Chem. Soc*. **1994**, *116*, 1165.

(7) Crooker, J. C.; Murray, R. W. *Anal. Chem.* **2000**, *72*, 3245.

(8) Nicholson, R. S. *Anal.Chem*. **1965**, *37*, 1351−1355.

(9) Porat, Z.; Crooker, J. C.; Zhang, Y.; Le Mest, Y.; Murray, R. W. *Anal. Chem.* **1997**, *69*, 5073.

(10) The authors thank O. Niwa of NTT, Japan, for these electrode materials.

(11) In all potential step experiments, current−time data are taken only well after the observed rise time of the electrode/melt cell. Our previous study[7] established that while iR_{unc} effects are present in cyclic voltammetry, they are minor contributors to peak potential separations (ΔE_{peak}), relative to slow electron-transfer rates.

(12) Williams, M. E.; Crooker, J. C.; Pyati, R.; Lyons, L. J.; Murray, R. W. *J. Am. Chem. Soc.* **1997**, *119*, 10249.

(13) Finklea, H. O. *Electroanal. Chem.* **1996**, *19*, 109.

(14) Newton, M. D.; Sutin, N. *Annu. Rev. Phys. Chem*. **1984**, 35, 437.

(15) Böttger, H.; Bryksin, V. V. *Hopping Conduction in Solids*; VCH Publishers: Deerfield, FL, 1985; p 51.

(16) Williams, M. E.; Murray, R. W. *J. Phys. Chem. B* **2000**, *104*, 10699.

(17) Fu, Y.; Col, A. S.; Swaddle, T. W. *J. Am. Chem. Soc.* **1999**, *121*, 10410.

(18) Hubbard, A. T.; Anson, F. C. *Electroanal. Chem*. **1970**, *4*, 129.

(19) Daum, P.; Lenhard, J. R.; Rolison, D.; Murray, R. W. *J. Am. Chem. Soc*. **1980**, *102*, 4649.

(20) Hicks, J. F.; Zamborini, F. P.; Osisek, A. J.; Murray R. W. *J. Am. Chem. Soc*., in press.

(21) Marcus, R. A. *J. Chem. Phys*. **1965**, *43*, 679.

(22) Feldberg, S. W. *J. Electroanal. Chem.* **1986**, *198*, 1.